TAO, Vol. 14, No. 3, 335-342, September 2003

A One-body Model of the 1999 Chi-Chi, Taiwan, Earthquake

Jeen-Hwa Wang[1,*]

(Manuscript received 28 March 2003, in final form 5 June 2003)

ABSTRACT

An M_s7.6 Chi-Chi earthquake, which ruptured the Chelungpu fault, struck central Taiwan on 20 September 1999 at 17:47 p.m. GMT. Observed data and inversion results show remarkable differences in source properties between the northern and southern segments of the Chelungpu fault. In this study, the Chelungpu fault is divided into two individual segments, and each segment is approximated by a one-body spring-slider model in the presence of friction. Results show that the simple model can interpret the differences in displacements and predominant periods between the two segments. Meanwhile, the ground surface displacement of the fault is capable of reflecting behavior of the thoroughly ruptured area, consisting of numerous different asperities, while the predominant period is able to display the oscillations of a major asperity in the fault plane. However, based on ground surface data the simple model cannot explain the differences in velocities and accelerations between the two segments.

(Key words: One-body spring-slider model, Displacement, Velocity, Acceleration, Stress drop)

1. INTRODUCTION

The M_s7.6 Chi-Chi earthquake struck central Taiwan on 20 September 1999 at 17:47 p.m. GMT (Ma et al. 1999; Shin 2000). The earthquake resulted from an over 80-kilometer-long, east-dipping thrust fault (that is, the Chelungpu fault), with a maximum vertical ground displacement of over 6 meters and with a maximum horizontal ground displacement of over 9 meters.

Since the occurrence of the Chi-Chi earthquake, numerous seismological, geophysical, geodetic, and geological observations have been made. All the results show remarkable differences in source properties between the northern and southern segments of the Chelungpu fault.

[1] Institute of Earth Sciences, Academia Sinica, Taipei, Taiwan, ROC

[*] *Corresponding author address*: Prof. Jeen-Hwa Wang, Institute of Earth Sciences, Academia Sinica, P. O. Box 1-55, Nangang, Taipei, Taiwan, ROC; E-mail: jhwang@earth.sinica.edu.tw

The two segments are almost separated at the middle of the fault. Tsai and Huang (1999) reported smaller near-fault peak ground accelerations (PGA) and larger near-fault peak ground velocities (PGV) at northern stations than those at southern ones. At near-fault stations, Wang et al. (2002) reported a lower degree of complexity of accelerograms and larger predominant periods at northern stations than at southern ones. They also stated that for the foot-wall stations there are only minor differences in the PGV values between the northern and southern stations, and the PGV at the hanging wall are generally larger than those at the foot wall. The difference in the PGA values at the hanging wall and the foot wall is small, and the PGA increases from north to south. Larger ground surface ruptures were in the northern segment than in the southern one (CGS 1999; Yu et al. 2001).

From the source rupture processes inverted from near-fault and teleseismic seismograms and GPS data, several investigators (Chi et al 2001; Kikuchi et al. 2000; Lee and Ma 2000; Ma et al. 2000, 2001; Wu et al. 2001; Zeng and Chen 2001) stated that larger-sized asperities and larger displacements occurred on the northern fault plane than on the southern one. Lee and Ma (1999) and Chen et al. (2001) reported lower rupture velocities on the northern fault plane than on the southern one. Although Hwang et al. (2001) and Huang et al. (2001) applied different methods to estimate stress drop from near-fault seismograms, they still obtained a similar conclusion-the stress drops at the northern stations are higher than those at the southern ones. From near-fault seismograms, Huang and Wang (2002) found that in the frequency range of 0.2-3 Hz, the displacement spectra, $P(\omega)$, follows power-law scaling: $P(\omega) \sim \omega^{-b}$, and the value of b changes from 3 at the northern segment to 2 at the southern one.

It is significant to explore possible causes that produce such differences in source properties between the northern and southern segments of the Chelungpu fault. In this study, an attempt is made to apply a one-body spring-slider model to approximate each segment of the Chelungpu fault and to investigate the differences in stress drops, predominant periods, displacements, velocities, and accelerations at the two segments.

2. MODEL

From the source rupture processes inferred by several authors (Chi et al. 2001; Kikuchi et al. 2000; Lee and Ma 2000; Ma et al. 2000, 2001; Wu et al. 2001; Zeng and Chen 2001), the whole fault plane is composed of asperities with different sizes and displacements: larger asperities with large displacements on the northern plane and smaller asperities with small displacements on the southern plane. Thus, although the Chelungpu fault is not disconnected geologically, it is still rational to divide the whole fault into two equal-length segments due to the above-mentioned differences in several source parameters. Each segment of the Chelungpu fault is approximated by an individual one-body spring-slider model (see Fig. 1). The two sliders related to the two segments are not connected to each other and move independently. Each slider with mass m is pulled by a leaf spring of strength, K, on a moving plate with a constant velocity, V_p. The motions of the slider are controlled by a frictional force, F. Thus, the equation of motion of the system is:

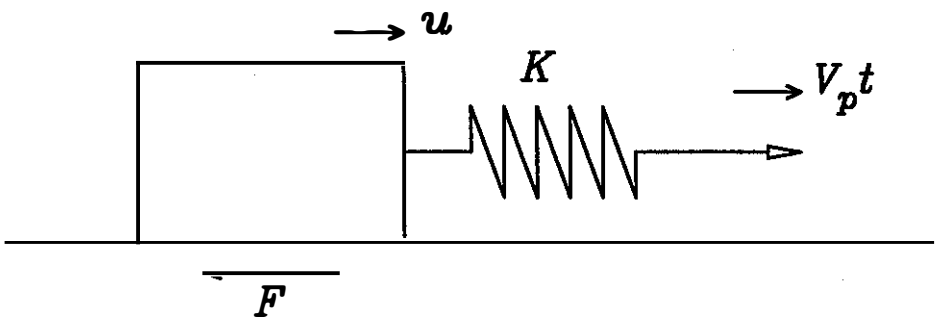

Fig. 1. One-body spring-slider model. In the figure, u, K, V_p, and F denote, respectively, the displacement, the spring constant, the velocity of the driving force, and the frictional force.

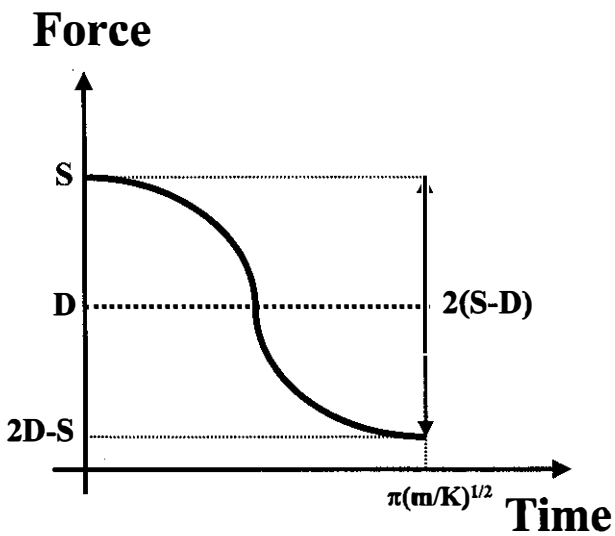

Fig. 2. The temporal variation of the force exerted on the slider. In the figure, S, D, 2D-S, 2(S-D), and $\pi (m/K)^{1/2}$ are, respectively, the static friction force, the dynamic friction force, the final force, the force drop, and the natural period of the system.

$$md^2u/dt^2 = -K(u - V_p t) - F. \quad (1)$$

Since the slider only moves along a single direction, the model can only assist us to study some aspects of observations and cannot give us a comprehensive solution. The static friction strength between the slider and the moving plate is denoted by S. When the driving force, i.e., $KV_p t$, which increases with time, is slightly larger than S, F changes from static friction strength to dynamic one, D, which is usually smaller than S. The friction law, which controls the variation

of friction with slip or velocity, is usually complicated (cf. Wang 2002). In order to simplify the problem and to study the primary problems, F in Eq. (1) changes immediately from S to D. Hence, the equation of motion becomes:

$$md^2u/dt^2 = -Ku + (S-D). \quad (2)$$

The solution of Eq. (2) is

$$u(t) = [(S-D)/K][1-\cos(2\pi t/T_n)], \quad (3)$$

where $T_n = 2\pi(m/K)^{1/2}$ is the natural period of the model. For a real earthquake, the predominant period of related seismograms can be considered to be the natural period of a related asperity on the ruptured fault plane. From Eq. (3), the force exerted on the slider is equal to $m(d^2u/dt^2) = (S-D)\cos(2\pi t/T_n)$. As shown in Fig. 2, the force varies from S to 2D-S, which is smaller than D, because of overshot after the slider moves. The drop of F from S to 2D-S leads to a force drop, that is, $\Delta F = S-(2D-S) = 2(S-D)$. Here, we consider the force drop to be the stress drop, $\Delta\sigma$, times the contact area, A, between the slider and the moving plate, that is, $\Delta F = A\,\Delta\sigma$. This leads to $\Delta\sigma = \Delta F/A = 2(S-D)/A$.

From Eq. (3), the peak displacement is $u_{max} = 2(S-D)/K = \Delta F/K$ when $\cos(2\pi t/T_n) = -1$, and is not a function of the mass of the slider. From Eq. (3), the velocity of the slider is $v(t) = du/dt = (\Delta F/2K)(2\pi/T_n)\sin(2\pi t/T_n)$ and the peak velocity is thus $v_{max} = (\Delta F/2K)(2\pi/T_n) = u_{max}(2\pi/T_n)$. The acceleration of the slider is $a(t) = d^2u/dt^2 = (\Delta F/2K)(2\pi/T_n)^2\cos(2\pi t/T_n)$ and the peak acceleration is thus $a_{max} = (\Delta F/2K)(2\pi/T_n)^2 = (u_{max}/2)(2\pi/T_n)^2$. For the Chelungpu fault, the relevant parameters are denoted by the following symbols: m_N, T_{nN}, $\Delta\sigma_N$, K_N, A_N, u_{maxN}, v_{maxN}, and a_{maxN} for the northern segment, and m_S, T_{nS}, $\Delta\sigma_S$, K_S, A_S, u_{maxS}, v_{maxS}, and a_{maxS} for the southern one. In order to compare the differences in source parameters between the two segments of the Chelungpu fault, several ratios of source parameters are defined as below: $u_{maxN}/u_{maxS} = (\Delta F_N/\Delta F_S)(K_S/K_N)$, $(\Delta F_N/\Delta F_S) = (\Delta\sigma_N/\Delta\sigma_S)(A_N/A_S)$, $v_{maxN}/v_{maxS} = (u_{maxN}/u_{maxS})(T_{nN}/T_{nS})$, $a_{maxN}/a_{maxS} = (u_{maxN}/u_{maxS})(T_{nN}/T_{nS})^2$, and $T_{nN}/T_{nS} = (m_N/m_S)^{1/2}(K_S/K_N)^{1/2}$.

3. DISCUSSION

Undoubtedly, it will be more significant if we can estimate the above-mentioned ratios from the data directly measured at the center of the fault plane of each segment. However, at present we only have the data observed on the ground surface and those just inferred from inversion results. In this study, we mainly use the data directly measured on the ground surface. For the purpose of comparison, the inversion results are also taken into account, even though their uncertainty is high. Based on ground surface data, we can, at least, obtain the low bound of information. The ratios estimated from the ground surface observations are denoted by a subscript "o" in the followings.

The ratio $(u_{maxN}/u_{maxS})_o$ is about 3 estimated from observed ground surface displacements (Yu et al. 2001). On the other hand, the ratio u_{maxN}/u_{maxS} estimated from the inverted slip distri-

butions on the fault plane by several authors (Chi et al. 2001; Kikuchi et al. 2000; Lee and Ma 1999; Ma et al. 2000, 2001; Wu et al. 2001; Zeng and Chen 2001) vary from 3 to 5. Since the surface ratio might be a lower limit of the ratio, the value of $(u_{maxN}/u_{maxS})_o \cong 3$ can be used for further studies. The results obtained by Huang et al. (2001) and Hwang et al. (2001) give $(\Delta\sigma_N/\Delta\sigma_S)_o \cong 2.5$. The studies by Wang et al. (2002) show (1) $(T_{nN}/T_{nS})_o \cong 5$ for all near-fault stations in both sides of the fault; and (2) $(v_{maxN}/v_{maxS})_o \cong 1$ and $(a_{maxN}/a_{maxS})_o \cong 0.5$ for the near-fault stations just on the foot-wall side. The values of several ratios obtained from the observations and inversions by several investigators are shown in Table 1. As mentioned above, the velocities and accelerations in the hanging wall are, on the average, much larger than those in the foot wall. However, in the southern segment there are no near-fault seismic data in the hanging wall. Thus, the value of $(v_{maxN}/v_{maxS})_o$ will be much larger than 1 and that of $(a_{maxN}/a_{maxS})_o$ smaller than 0.5 when the peak velocities on the hanging wall are taken into account. By using the data recorded both at the hanging wall and at the foot wall, Tsai and Huang (1999) and Brodsky and Kanamori (2002) concluded large differences in the velocities between the northern and southern segments of the Chelungpu fault. Brodsky and Kanamori (2002) also proposed a lubrication model to interpret the difference. This must be inappropriate, because from numerical simulations Huang et al. (2002) claimed large differences in the velocities between the hanging and footing walls due to geological structures. It is better to estimate the ratio just based on seismic data recorded only at either the hanging-wall stations or the foot-wall ones. Hence, in the followings only the ratios $(v_{maxN}/v_{maxS})_o$ and $(a_{maxN}/a_{maxS})_o$ estimated from the foot-wall seismic data are used.

Based on the previous theoretical results, $(u_{maxN}/u_{maxS})_o \cong 3$ and $(\Delta\sigma_N/\Delta\sigma_S)_o \cong 2.5$ lead to $(\Delta F_N/\Delta F_S)_o(K_S/K_N) = (\Delta\sigma_N/\Delta\sigma_S)_o(A_N/A_S)(K_S/K_N) \cong 2.5(A_N/A_S)(K_S/K_N) \cong 3$. Although the values of A_N/A_S and K_S/K_N are not exactly known, it is still possible to estimate their values from related information. The value of known K_S/K_N depends upon the degree of coupling between the moving plate and the fault zone. For the two segments belong to the same tectonic province, coupling could be essentially similar for both northern and southern segments. Hence, we can assume $K_S \cong K_N$. This leads to $A_S \cong A_N$. Several investigators (Chi et al. 2001; Kikuchi et al. 2000; Lee and Ma 1999; Ma et al. 2000, 2001; Wu et al. 2001; Zeng and Chen 2001) showed that the ruptured areas of northern and southern segments of the Chelungpu fault are almost equal and almost a half of the whole rupture area, that is, $A_N/A_S \cong 1$. Obviously, the ratio of ruptured areas estimated from the ground surface displacements is similar to that obtained from source inversion. This might imply that the ground surface displacement is associated with the movement of the whole ruptured area, which consists of numerous different asperities. For comparison, if we use the maximum displacements obtained from inverted results, i.e., $(u_{maxN}/u_{maxS}) \cong 5$, the estimated value of A_N/A_S is about 2. In addition, the above-mentioned studies indicated large ruptures in the northern fault plane extended from the ground surface to a depth of about 20 km, while those in the southern one did only from the ground surface to 10 km and the displacements are very small at a depth larger than 10 km. Hence, the major ruptured area in the former is about twice larger than that in the latter. This can conform the estimation.

On the other hand, the value of (A_N/A_S) can also be estimated from the ratio of the northern predominant period to the southern one, i.e., T_{nN}/T_{nS}. The value of $(T_{nN}/T_{nS})_o \cong 5$ gives $(m_N/$

Table 1. The approximative average values of several ratios obtained from observations and inversions made by several investigators as mentioned in the text. The value with subscript "o" denotes that obtained from surface observations, while the value without subscript "o" shows that from inversions.

Ratio	Approximated values
$(u_{maxN}/u_{maxS})_o$	3
u_{maxN}/u_{maxS}	3-5
$(v_{maxN}/v_{maxS})_o$	1
$(a_{maxN}/a_{maxS})_o$	0.5
$(T_{nN}/T_{nS})_o$	5
$(\Delta\sigma_N/\Delta\sigma_S)_o$	2.5

$m_S)(K_S/K_N) = (\rho_N h_N A_N/\rho_S h_S A_S)(K_S/K_N) = (T_{nN}/T_{nS})_o^2 \cong 25$, where the symbols ρ and h denote, respectively, the density and average height of seismogenic zone. As mentioned above, the geological structures and sizes of the northern and southern portions of the source region are almost the same, and, thus, it is plausible to assume $\rho_N = \rho_S$ and $h_N = h_S$. This gives $(A_N/A_S)(K_S/K_N) \cong 25$, thus leading to $(A_N/A_S) \cong 25$ because of $K_S \cong K_N$ as mentioned above. This indicates that the ratio is about 25 times larger than that estimated from the ground surface displacements. The predominant period of the seismograms recorded at a station near a major ruptured asperity (or a sub-event) could be considered to be the natural period associated with the oscillation of such an asperity. Hence, the predominant period is related to the oscillation of a major asperity in the ruptured area. The source rupture processes inverted by several authors, as mentioned above, show that the asperity in the northern fault plane is actually much larger than that in the southern one. The inversion result confirms the conclusion.

The observed value of $(u_{maxN}/u_{maxS})_o \cong 3$ leads to a fact that the value of $\Delta F_N/\Delta F_S = (u_{maxN}/u_{maxS})_o(K_S/K_N)$ is about 3, because of $K_S/K_N \cong 1$. In other words, the average force drop in the northern fault plane is about 3 times larger than that in the southern one. This means that it takes longer time, at least 3 times, to drive the extra tectonic force to reach the static friction force for generating next event in the northern segment than in the southern one. Hence, the recurrence time of the northern segment might be, at least, 3 times longer than that of the southern one. If we use the maximum displacements obtained from inverted results, i.e., $(u_{maxN}/u_{maxS}) \cong 5$, the estimated value of $\Delta F_N/\Delta F_S$ is about 5. This indicates that the recurrence time of the northern segment might be, at least, 5 times longer than that of the southern one. The undergoing paleoseismicity study along the Chelungpu fault will provide significant information to resolve the problem.

Theoretically, it is possible to estimate the ratios of both PGV and PGA from the ratios of both displacement and predominant period. The observed values of $(u_{maxN}/u_{maxS})_o \cong 3$ and $(T_{nN}/T_{nS})_o \cong 5$ yield the estimated values of $v_{maxN}/v_{maxS} \cong 3/5 = 0.6$ and $a_{maxN}/a_{maxS} \cong 3/5^2 = 0.12$.

Obviously, the two estimated values are, respectively, smaller than the observed ones of $(v_{maxN}/v_{maxS})_o \cong 1$ and $(a_{maxN}/a_{maxS})_o \cong 0.5$. This indicates that based on the ground surface displacements, the model with two independent sliders cannot completely explain the observed velocities and accelerations. On the other hand, if we use the maximum displacements obtained from inverted results, i.e., $(u_{maxN}/u_{maxS}) \cong 5$, the estimated values of v_{maxN}/v_{maxS} and a_{maxN}/a_{maxS} are about 1 and 0.5, respectively, which are similar to the observed ones. Results seem to indicate that the ground surface displacement is only capable of showing average behavior of the rupture area as mentioned previously, while the velocity and acceleration are able to reflect the properties of the main ruptured area.

4. CONCLUSIONS

The results based on a simple model with two independent sliders, in the presence of friction, show that the displacement is capable of reflecting behavior of a ruptured area, which consists of numerous different asperities, while the predominant (or natural) period is able to display the oscillation of the major asperity on the fault plane. However, based on the ground displacements the simple model cannot interpret the differences in velocities and accelerations between the northern and southern segments of the Chelungpu fault. In order to understand the overall behavior of the fault, we need (1) accurate directly measured data and/or inverted results in the fault zone; and (2) a more comprehensive model consisting, at least, of two coupled sliders in the presence of a more complicated friction force. Wang (1995) stressed the importance of coupling between two sub-faults on earthquake ruptures.

Acknowledgments The author thanks two anonymous reviewers for their useful comments. The study was financially supported by Academia Sinica and the National Sciences Council under grant No. NSC91-2119-M-001-020.

REFERENCES

Brodsky, E. E., and H. Kanamori, 2001: Elastohydrodynamic lubrication of faults. *J. Geophys. Res.*, **106**, 16357-16374.

CGS, 1999: Geological Survey of the 921 Earthquake (in Chinese), Open-File Rept. *Central Geological Survey, MOEA, ROC*, 315pp.

Chen, K. C., B. S. Huang, W. G. Huang, J. H. Wang, T. M. Chang, R. D. Hwang, H. C. Chiu, and C. C. Tsai, 2001: An observation of rupture pulses of the 20 September 1999, Chi-Chi, Taiwan, earthquake from near-field seismograms. *Bull. Seism. Soc. Am.*, **91**, 1247-1254.

Chi, W. C., D. Dreger, and A. Kaverina, 2001: Finite-source modeling of the 1999 Taiwan (Chi-Chi) earthquake derived from a dense strong-motion network. *Bull. Seism. Soc. Am.*, **91**, 1144-1157.

Huang, B. S., K. C. Chen, W. G. Huang, J. H. Wang, and T. M. Chang, 2001: Numerical modeling for near-source strong ground motions of the 20 September 1999, Chi-Chi, Taiwan, earthquake. *J. Chin. Inst. Engin. Series A*, **25**, 437-446.

Huang, M. W., and J. H. Wang, 2002: Scaling of displacement spectra of the 1999 Chi-Chi, Taiwan, earthquake from near-fault seismograms. *Geophys. Res. Lett.*, **29**, 47:1-4.

Huang, W. G., J. H. Wang, B. S. Huang, K. C. Chen, R. D. Hwang, T. M. Chang, R. D. Huang, H. C. Chiu, and C. C. Tsai, 2001: Estimates of source parameters for the Chi-Chi, Taiwan, earthquake based on Brune's source model. *Bull. Seism. Soc. Am.*, **91**, 1190-1198.

Hwang, R. D., J. H. Wang, B. S. Huang, K. C. Chen, W. G. Huang, D. M. Chang, R. D. Huang, H. C. Chiu, and C. C. Tsai, 2001: Estimates of stress drop from near-field seismograms of the M_s7.6 Chi-Chi, Taiwan, earthquake of 20 September 1999. *Bull. Seism. Soc. Am.*, **91**, 1158-1166.

Kikuchi, M., Y. Yagi, and Y. Yamanaka, 2000: Source process of the Chi-Chi, Taiwan, earthquake of 21 September 1999 inferred from teleseismic body waves. *Bull. Earthquake Res. Inst., Univ. Tokyo*, **75** (Part 1), 1-14.

Lee, S. J., and K. F. Ma, 2000: Rupture process of the 1999 Chi-Chi, Taiwan, earthquake from the inversion of teleseismic data. *TAO*, **11**, 591-608.

Ma, K. F., C. T. Lee, Y. B. Tsai, T. C. Shin, and J. Mori, 1999: The Chi-Chi, Taiwan, earthquake: large surface displacements on an island thrust. *EOS*, AGU, **80**, 605-611.

Ma, K. F., Song, T. R. Song, S. J. Lee, and H. I. Wu, 2000: Spatial slip distribution of the 20 September 1999, Chi-Chi, Taiwan, earthquake (M_w7.6): Inverted from teleseismic data. *Geophys. Res. Lett.*, **27**, 3417-3420.

Ma, K. F., J. Mori, S. J. Lee, and S. B Yu, 2001: Spatial and temporal slip distribution of the Chi-Chi, Taiwan, earthquake from strong motion, teleseismic and GPS data. *Bull. Seism. Soc. Am.*, **91**, 1069-1087.

Shin, T. C., 2000: Some seismological aspects of the 1999 Chi-Chi earthquake in Taiwan. *TAO*, **11**, 555-566.

Tsai, Y. B., and M. W. Huang, 1999: Strong ground motion characteristics of the Chi-Chi, Taiwan, earthquake of 21 September 1999. *Earthquake Engng. Engng. Seism.*, **2**, 1-21.

Wang, J. H., 1995: Effect of seismic coupling on the scaling of seismicity. *Geophys. J. Intl.*, **121**, 475-488.

Wang, J. H., 2002: A dynamical study of two one-variable, rate-dependent, and state-dependent friction laws. *Bull. Seism. Soc. Am.*, **92**, 687-694.

Wang, J. H., M. W. Huang, K. C. Chen, R. D. Hwang, and W. Y. Chang, 2002: Aspects of characteristics of ground motions of the 1999 Chi-Chi (Taiwan) earthquake. *J. Chin. Engin. Soc., Series A*, **25**, 507-519.

Wu, C., M. Takeo, and S. Ide, 2001: Source Process of the Chi-Chi earthquake: A joint inversion of strong motion data and global positioning system data with a multifault model. *Bull. Seism. Soc. Am.*, **91**, 1128-1143.

Yu, S. B., L. C. Kuo, Y. J. Hsu, H. H. Su, C. C. Liu, C. S. Hou, J. F. Lee, T. C. Lai, C. C. Liu, C. L. Liu, T. F. Tseng, C. S. Tsai, and T. C. Shin, 2001: Pre-seismic deformation and co-seismic displacements associated with the 1999 Chi-Chi, Taiwan, earthquake. *Bull. Seism. Soc. Am.*, **91**, 995-1012.

Zeng, Y. H., and C. H. Chen, 2001: Source inversion of the 1999 Chi-Chi earthquake, Taiwan with the composite source model. *Bull. Seism. Soc. Am.*, **91**, 1088-1098.